AGU PUBLICATIONS

Geophysical Research Letters

RESEARCH LETTER
10.1002/2016GL070065

Key Points:
- Earth and Titan exhibit contrasting precession responses because of their different rotation rates
- For Titan, length of summer controls hemispheric asymmetries of the precipitation response
- For Earth, maximum insolation controls hemispheric asymmetries of the precipitation response

Supporting Information:
- Supporting Information S1

Correspondence to:
T. Schneider,
tapio@caltech.edu

Citation:
Liu, J., and T. Schneider (2016), Contrasting responses to orbital precession on Titan and Earth, *Geophys. Res. Lett.*, *43*, 7774–7780, doi:10.1002/2016GL070065.

Received 8 APR 2016
Accepted 15 JUL 2016
Accepted article online 19 JUL 2016
Published online 30 JUL 2016
Corrected 12 AUG 2016

This article was corrected on 12 AUG 2016. See the end of the full text for details.

Contrasting responses to orbital precession on Titan and Earth

Junjun Liu[1] and Tapio Schneider[1,2]

[1]California Institute of Technology, Pasadena, California, USA, [2]ETH Zurich, Zurich, Switzerland

Abstract Earth and Titan exhibit contrasting atmospheric responses to orbital precession. On Earth, most (water) precipitation falls in low latitudes, and precipitation is enhanced in a hemisphere when perihelion occurs in that hemisphere's summer. On Titan, most (methane) precipitation falls in high latitudes, and precipitation is enhanced in a hemisphere when aphelion occurs in that hemisphere's summer. We use a Titan general circulation model to elucidate the dynamical reasons for these different responses to orbital precession. They arise primarily because of the different diurnal rotation rates of Titan and Earth. The slower rotation rate of Titan leads to wider Hadley cells that transport moisture into polar regions. Changes in the length of summer, rather than in the intensity of summer insolation as in Earth's tropics, then dominate the precession response of the hydrologic cycle.

1. Introduction

Saturn's moon Titan is the only planetary body in our solar system that has an analog of Earth's hydrologic cycle. Like water on Earth, methane on Titan evaporates at the surface, is transported through the atmosphere, and precipitates back to the surface. Titan and Earth also have similar orbital eccentricity and obliquity, and both exhibit orbital variations. In particular, their perihelion—the time of year when the planet is closest to the Sun—precesses on timescales of tens of thousands of years. Yet their responses to orbital precession are very different: On Earth, most (water) precipitation occurs in low latitudes [e.g., *Schneider et al.*, 2014], and paleoclimate proxies indicate that annual-mean net precipitation is enhanced in a hemisphere when perihelion occurs during summer in that hemisphere—that is, in the hemisphere that has the brighter summer with more intense insolation [e.g., *Cruz*, 2005; *Wang et al.*, 2006, 2007, 2008; *Herzschuh*, 2006]. On Titan, by contrast, data from the Cassini spacecraft have shown that hydrocarbon lakes mainly occur in polar regions, preferentially in the north [*Aharonson et al.*, 2009], and this hemispheric dichotomy in the lake distribution is thought to be driven by a north-south asymmetry in the (methane) precipitation distribution that arises from Saturn's orbital eccentricity [*Schneider et al.*, 2012; *Lora et al.*, 2014; *Lora and Mitchell*, 2015]. Currently, perihelion occurs during Titan's (or Saturn's) southern hemisphere summer (like on Earth today), so the northern summer is dimmer than the southern. Accumulation of methane in the north polar region therefore may seem puzzling, given that precipitation on Earth is enhanced in the hemisphere with the brighter summer. That precipitation is enhanced in the hemisphere with the brighter summer is usually taken as axiomatic [e.g., *Ruddiman*, 2013].

Key to understanding the contrasting precession responses is that orbital eccentricity leads not only to seasonal variations of the intensity of insolation but also to variations in the length of seasons. At perihelion, insolation is most intense, but the orbital angular velocity is also maximal, shortening the season during which perihelion occurs. Conversely, at aphelion, insolation is least intense, but the orbital angular velocity is minimal, lengthening the season during which aphelion occurs. Because Titan's (or Saturn's) perihelion currently occurs in southern summer, the southern summer is not only brighter but also shorter than the northern summer. The effects of length-of-season variations and insolation variations between perihelion and aphelion exactly balance each other when integrated over a season, so annual-mean insolation is not affected by precession of the longitude of perihelion. Therefore, if the response of methane net precipitation (precipitation minus evaporation) were linear in insolation, annual-mean net precipitation would be symmetric between the northern and southern hemispheres, barring any sizable influence of asymmetries in surface boundary conditions. But simulations with a Titan general circulation model (GCM) show that even without asymmetries in surface boundary conditions and consistent with the observed preferential hydrocarbon accumulation in the north, more annual-mean net precipitation occurs in the northern hemisphere, preferentially in the north polar region in summer—apparently because the northern summer, albeit dimmer,

is currently longer [*Schneider et al.*, 2012; *Lora et al.*, 2014]. By contrast, enhanced annual-mean net precipitation in Earth simulations occurs in the hemisphere with the brighter summer [*Kutzbach and Guetter*, 1986], possibly because of correlations between insolation variations and the seasonal cycle of moisture advection [*Merlis et al.*, 2013b] and/or because of nonlinear dynamical effects of continents on the mean circulation [*Tigchelaar and Timmermann*, 2015].

Here we use a Titan GCM to show that the different responses to orbital precession principally arise because of the differences in Titan's and Earth's diurnal rotation rates: Titan's rotation rate is only 1/16 of Earth's. The different rotation rates imply differences in the width of the Hadley cells and their meridional reach in transporting moisture (water or methane) [*Held and Hou*, 1980; *Walker and Schneider*, 2005; *Schneider*, 2006; *Mitchell et al.*, 2006]. These differences in moisture transport, in turn, control the relative importance of the length of summer and intensity of summer insolation in determining the atmospheric responses to orbital precession.

2. Model Setup

The Titan GCM is based on the Flexible Modeling System of the Geophysical Fluid Dynamics Laboratory. It is similar to standard Earth models, but with Titan's physical parameters [*Schneider et al.*, 2012]. It is a spectral transform model, and here we use T42 resolution in the horizontal (corresponding to about 2.5° × 2.5° resolution of the transform grid) and 18 unevenly spaced levels in the vertical (the uppermost level has a mean pressure of 15 mbar). Radiative transfer is represented using the two-stream approximation. Solar radiation is scattered and absorbed in the atmosphere, assuming diffuse incidence and multiple scattering. Long-wave radiation is absorbed in the atmosphere. Parameters in the relatively simple representation of radiative transfer are chosen so that the modeled radiative fluxes match observations, similar to *Schneider et al.* [2012] but correcting errors in the implementation of the radiative transfer scheme in that earlier study (see the supporting information). Surface hydrology is represented by a bucket model [*Manabe*, 1969], with surface methane flows represented crudely (and somewhat unrealistically) as diffusive. See the supporting information for model details.

The simulations are initialized with a dry surface and with an isothermal (86 K) atmosphere containing the equivalent of 12 m of liquid methane distributed uniformly. The total methane concentration is conserved in the simulations, up to negligibly small numerical inaccuracies. In the statistically steady state that is reached after a long spin-up period (100 Titan years, with 1 Titan year = 10,758 Earth days), the seasonally and globally averaged methane concentration in the atmosphere corresponds to ∼8 m liquid methane in the simulations with Titan's rotation rate and to ∼7.5 m in the simulation with Earth's rotation rate. The remaining methane is on the surface. The results we show are averages over 20 Titan years in this statistically steady state.

To investigate the effects of the rotation rate, we conducted four simulations: two simulations with Titan's rotation rate, for perihelion in southern summer (with Titan's current longitude of perihelion $\varpi = 277.7°$) and for the longitude of perihelion turned by 180° ($\varpi = 97.7°$), and two simulations with Earth's rotation rate, for longitudes of perihelion $\varpi = 277.7°$ and 97.7°. (Because of the hemispheric symmetry of the boundary conditions, turning the longitude of perihelion by 180° reflects hemispheric asymmetries in the annual-mean climate about the equator, provided that multiple statistical equilibria cannot occur simultaneously. To be sure that the hemispheric asymmetries that develop in our simulations are indeed unique statistical equilibria, we run separate simulations with the longitude of perihelion turned by 180°.) All other parameters are kept fixed.

3. Results

The simulations with different rotation rates exhibit drastically different responses to precession. For the simulation with Titan's rotation rate and perihelion in southern summer ($\varpi = 277.7°$), methane accumulates in the polar regions, with a preference for the north (Figure 1, first row). This is consistent with the observed hydrocarbon lake distribution [*Aharonson et al.*, 2009] and previous simulations [*Schneider et al.*, 2012; *Lora et al.*, 2014, 2015; *Lora and Mitchell*, 2015]. Integrated over the polar caps bounded by 60°N/S, the mean surface methane coverage is 37.4 m in the north polar region versus 11.8 m in the south. (The precise polar methane coverage depends on the observationally poorly constrained amount of total methane in the system and the strength of the along-surface methane diffusion.) The equatorial region between 20°S and 20°N is relatively dry, with a mean methane coverage of ≤0.2 m. However, when the rotation rate is increased to Earth's, the hemispheric

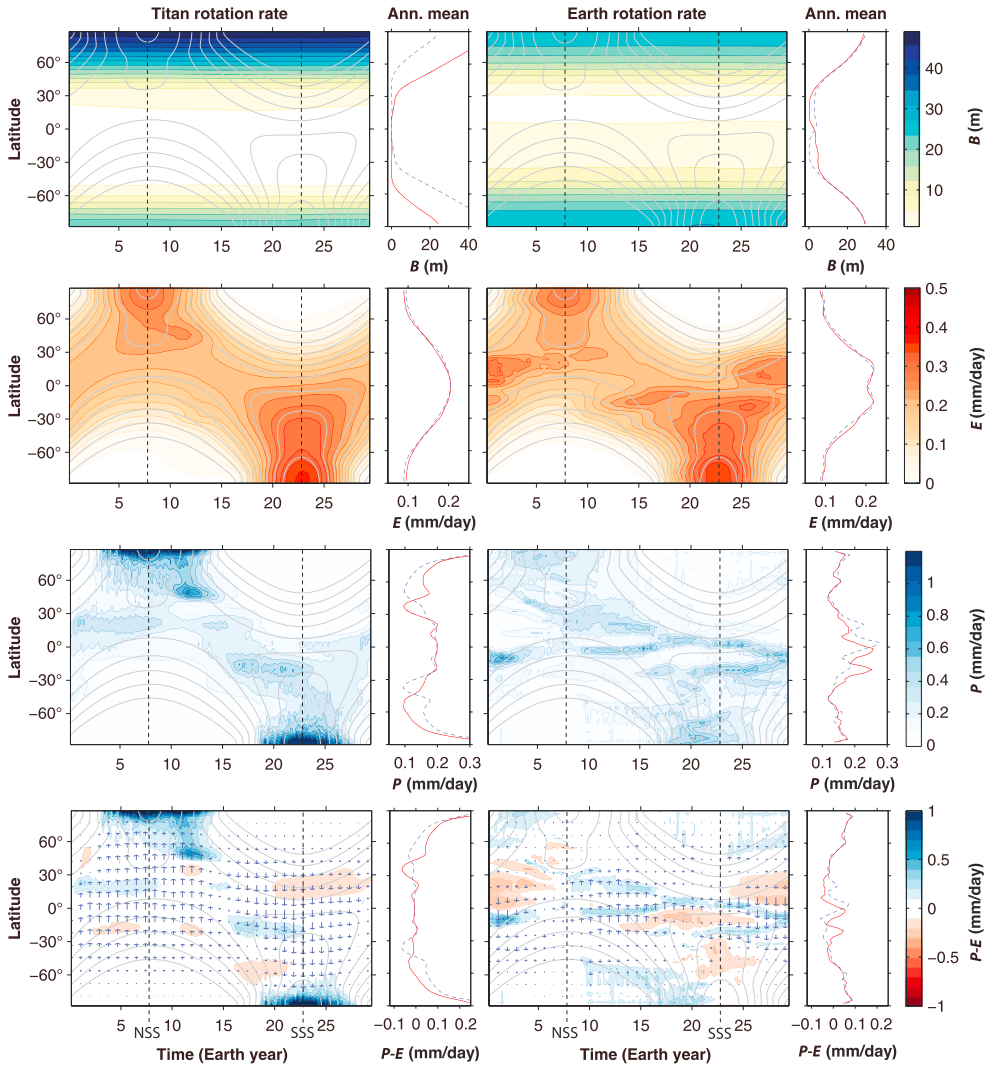

Figure 1. (top to bottom rows) Seasonal evolution of the methane surface reservoir B, evaporation E, precipitation P, and net precipitation $P - E$ for the simulations with Titan's rotation rate (left) and Earth's rotation rate (right), all with perihelion in southern summer ($\varpi = 277.7°$). The grey contours indicate the net solar flux at the surface (contour interval 0.1 W m^{-2}), and the dashed grey lines mark the northern summer solstice (NSS) and the southern summer solstice (SSS). The arrows in the $P - E$ plots show the column-integrated meridional methane flux. The panels on the right show the annual mean of the quantity in the contour plots (red lines), and the annual means for the simulations with perihelion in northern summer ($\varpi = 97.7°$) (blue lines), to be able to see the precession-induced changes clearly.

dichotomy in the high-latitude surface methane distribution nearly disappears (Figure 1, first row). Methane is evenly distributed between the two polar caps, each with mean methane coverage of ~23 m. Instead, the equatorial regions are less dry, with more methane accumulating in the south: about 3.6 m of methane accumulate in the southern equatorial region between 0° and 20°S versus 0.8 m in the northern equatorial region between 0° and 20°N.

The surface methane accumulation is controlled by the net precipitation, with precipitation differences (rather than evaporation differences as suggested by *Aharonson et al.* [2009]) between the hemispheres responsible for the hemispheric dichotomies. Since the thermal inertia of Titan's surface is small and evaporation is the dominant loss term balancing insolation in the surface energy budget (in our model as well as on Titan itself), evaporation follows insolation at the surface wherever surface methane is available to evaporate; this holds irrespective of the rotation rate (Figure 1, second row). Thus, like annual-mean insolation, annual-mean evaporation is essentially symmetric between the two hemispheres; it has similar structures and magnitudes for Titan's and Earth's rotation rate. By contrast, annual-mean precipitation exhibits hemispheric asymmetries

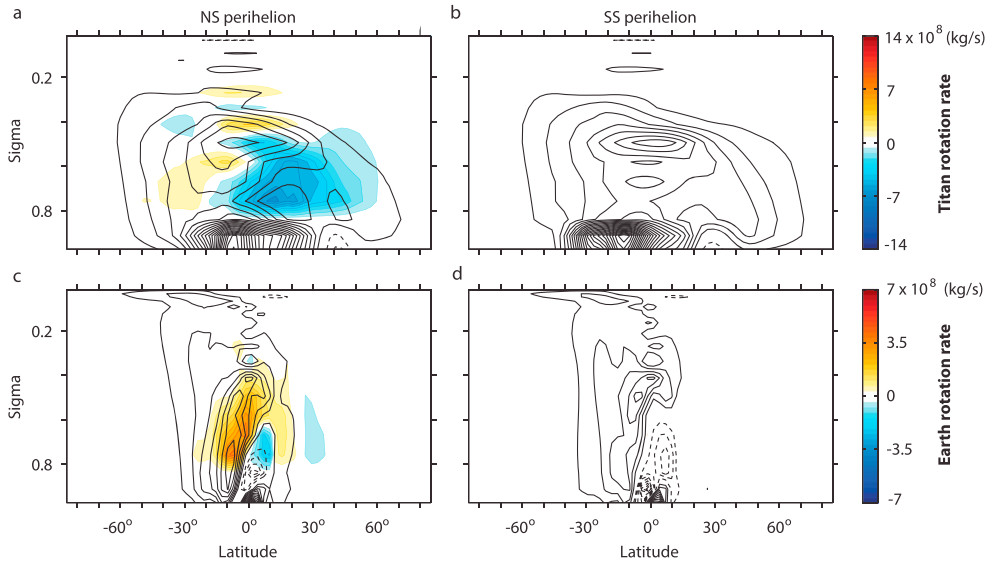

Figure 2. Stream function (contours) of the mean meridional mass circulation averaged over northern spring and summer, i.e., from vernal equinox ($t = 0$) to autumnal equinox ($t = 0.5$ Titan year = 14.7 Earth years). (a, c) Simulations with perihelion in northern summer ($\varpi = 97.7°$). (b, d) Simulations with perihelion in southern summer ($\varpi = 277.7°$). Figures 2a and 2b show simulations with Titan's rotation rate; Figures 2c and 2d show simulations with Earth's rotation rate. Dashed contours for clockwise rotation; solid contours for anticlockwise rotation. The contour intervals are 2×10^8 kg s^{-1} for the simulations with Titan's rotation rate and 0.75×10^8 kg s^{-1} for the simulations with Earth's rotation rate. Colors show the difference in the stream function strength between the simulations with perihelion in northern summer ($\varpi = 97.7°$, left) and in southern summer ($\varpi = 277.7°$, right). Colors are shown only above the boundary layer ($\sigma < 0.84$). (The stream function intersects the surface because it is a seasonal mean, for which time tendencies of surface pressure are not zero.)

and substantial differences between simulations with Titan's and Earth's rotation rates (Figure 1, third row). For Titan's rotation rate, mean precipitation is strongest in the polar regions. This leads to positive net precipitation in polar regions, balanced by negative net precipitation in lower latitudes and methane transport along the surface (Figure 1, fourth row). With Titan's current longitude of perihelion, the annually integrated net precipitation averaged over the polar caps bounded by 60°N/S is 0.93 m in the north versus 0.44 m in the south; most of the additional 0.5 m of net precipitation in the north comes from additional precipitation. When the rotation rate is increased to Earth's, annual-mean precipitation in the polar regions is similar in the north and south, and it is similar to evaporation, leading to small net precipitation in polar regions (Figure 1, fourth row). However, in the equatorial region, annual-mean precipitation is 0.5 m greater in the southern equatorial region (0 to 20°S) than in the northern equatorial region (0 to 20°N). This is responsible for the surface methane accumulation in the southern equatorial region.

What leads to any net precipitation is the atmospheric meridional methane transport, which, in the annual mean, is balanced by the methane transport along the surface. For Titan's rotation rate, the atmospheric meridional methane transport around the solstices reaches deep into the polar region of the summer hemisphere (Figure 1, fourth row). For Earth's rotation rate, by contrast, atmospheric meridional methane transport is largely confined to the equatorial region. In either case, the methane transport at any time of year is dominated by the mean meridional circulation (MMC); eddy transports are weaker in every season (Figure S3 in the supporting information). However, in the annual mean, eddy transports are comparable with MMC transports in low latitudes in the simulations with Titan's rotation rate and are stronger than MMC transports in polar regions in the simulations with Earth's rotation rate, because of partially canceling seasonal contributions by the MMC. For Titan's rotation rate, the MMC (Hadley circulation) around the solstices reaches from the summer to the winter polar region, with the near-surface flow transporting methane from the winter hemisphere deep into the summer hemisphere (Figures 2a and 2b). For Earth's rotation rate, by contrast, the Hadley circulation is confined to the equatorial region between 30°S to 30°N (Figures 2c and 2d). This difference between the simulations is consistent with the theoretical expectation that the width of the Hadley circulation increases

as the rotation rate decreases [*Held and Hou*, 1980; *Walker and Schneider*, 2006; *Schneider*, 2006; *Mitchell et al.*, 2006]. The difference is crucial for understanding the differences between the simulations mechanistically.

4. Mechanisms

In a statistically steady state, atmospheric methane transport balances net precipitation $P - E$ in the annual $\overline{(\cdot)}$ and zonal $[\cdot]$ mean, according to the atmospheric methane budget integrated over atmospheric columns,

$$[\overline{P} - \overline{E}] = -\int_0^{p_s} \frac{1}{r\cos\phi}\frac{\partial}{\partial\phi}\left(\cos\phi\left[\overline{vq}\right]\right)\frac{\mathrm{d}p}{g}. \tag{1}$$

Here ϕ is latitude, r the planetary radius, P the precipitation rate, E the evaporation rate, v meridional velocity, and q specific humidity. Because evaporation in the annual mean is essentially unaffected by precession (Figure 1), changes of the annual-mean atmospheric meridional methane flux $\delta\overline{vq}$ under precession are approximately balanced by changes of annual-mean precipitation $\delta\overline{P}$.

The response $\delta\overline{vq}$ of the atmospheric meridional methane flux to precession can be decomposed as [*Clement et al.*, 2004; *Held and Soden*, 2006; *Merlis et al.*, 2013b]

$$\delta\overline{vq} = \bar{q}\delta\bar{v} + \bar{v}\delta\bar{q} + \delta\bar{v}\delta\bar{q} + \delta\overline{v'q'}, \tag{2}$$

where $\bar{q}\delta\bar{v}$ is the dynamic component, $\bar{v}\delta\bar{q}$ is the thermodynamic component, $\delta\bar{v}\delta\bar{q}$ is the quadratic interaction term, and $\delta\overline{v'q'}$ represents changes in the transient eddy fluxes. The thermodynamic component $\bar{v}\delta\bar{q}$ represents changes of the specific humidity under precession, which are dominated by changes of the saturation specific humidity q_s: $\bar{v}\delta\bar{q} \approx \bar{v}\mathcal{H}\delta\bar{q}_s$ with relative humidity $\mathcal{H}$. By the Clausius-Clapeyron relation, changes of the saturation specific humidity are related to temperature changes δT through $\delta q_s/q_s \approx \alpha\delta T$, where $\alpha = \mathrm{d}\log(q_s)/\mathrm{d}T$ is the fractional rate of change of saturation specific humidity with temperature. Near Titan's surface, temperatures are around $T = 92$ K, giving $\alpha \approx 11\%\ \mathrm{K}^{-1}$ for methane; this is greater than $\alpha \approx 6.5\%\ \mathrm{K}^{-1}$ for water near Earth's surface in the tropics [*Held and Soden*, 2006; *Schneider et al.*, 2010]. However, the temperature changes under precession are very small (<1 K). Thus, changes of the thermodynamic component in response to precession end up being small: in our simulations both for Titan's and Earth's rotation rate, they are about one order of magnitude smaller than changes of the dynamic component $\bar{q}\delta\bar{v}$. This is different from simulations with Earth parameters, in which the thermodynamic component dominates over the dynamic component when the surface is water covered because precession-induced temperature variations are much larger than in the simulations with Titan parameters [*Merlis et al.*, 2013a, 2013b]. Similarly, the quadratic interaction term $\delta\bar{v}\delta\bar{q}$ and the changes in the transient eddy fluxes $\delta\overline{v'q'}$ are small relative to changes of the dynamic component in regions where substantial net precipitation changes under precession occur (see Figure S4 in the supporting information). However, although precession-induced changes in transient eddy moisture fluxes $\delta\overline{v'q'}$ are unimportant for shaping the $P-E$ response, eddy fluxes generally—of momentum and energy—are important for shaping the mean meridional circulation, as is well known generally [*Walker and Schneider*, 2005; *Schneider*, 2006] and has also been seen in Titan simulations [*Lora and Mitchell*, 2015].

Thus, the response of atmospheric methane fluxes to orbital precession is dominated by the dynamic component $\bar{q}\delta\bar{v}$, as in comprehensive Earth simulations [*Tigchelaar and Timmermann*, 2015]. The dynamic component represents the methane transport effect of the MMC response to precession. The MMC can change its strength and structure and in particular the latitude of its ascending branch. The latter is nonlinearly coupled to the strength through the angular momentum balance: A Hadley circulation generally strengthens as its ascending branch moves closer to the pole, with the strengthening being more nonlinear the closer the upper branch of the circulation is to the angular momentum-conserving limit [*Lindzen and Hou*, 1988; *Walker and Schneider*, 2005]. A brighter summer at perihelion can shift the ascending branch of the MMC toward the summer pole, nonlinearly strengthening the circulation and leading to enhanced moisture transport into the low-level convergence zone under the ascending branch. This occurs in the simulations with Earth's rotation rate: The ascending branch of the Hadley circulation shifts poleward in the brighter summer at perihelion (Figures 2c and 2d). As a consequence, the solstitial circulation and the upward mass flux in the northern equatorial region strengthen when perihelion occurs in northern summer (Figure 3b), resulting in the stronger moisture transport and enhanced net precipitation in the hemisphere with the brighter summer.

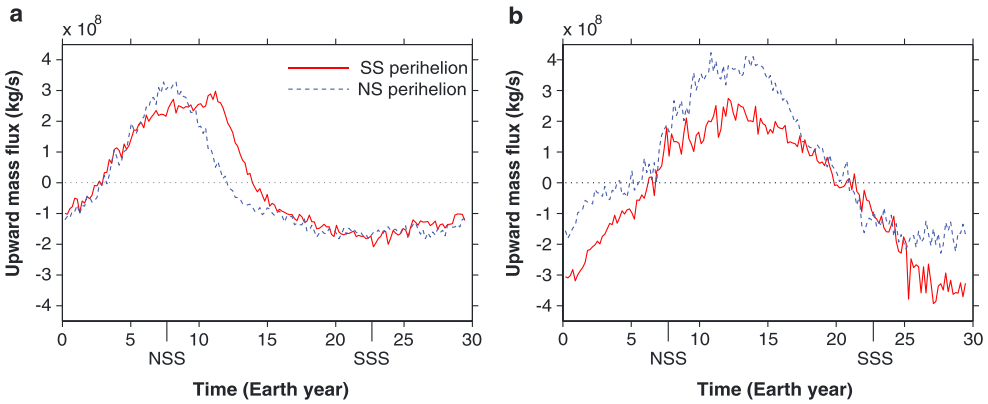

Figure 3. Upward mass flux (a) integrated over the polar region (poleward of 60°N) for Titan simulations and (b) integrated over the equatorial region from 0° to 30°N for Earth simulations. The upward mass flux is averaged in the upper atmosphere (above 4 km). Red for southern summer perihelion ($\varpi = 277.7°$) and blue for northern summer perihelion ($\varpi = 97.7°$).

The effect of the shortening of summer during perihelion is small in the equatorial region: the upward mass flux extends over a similar period in the equatorial region whether summer coincides with perihelion or aphelion (Figure 3b). Thus, the strengthening of the solstitial Hadley circulation dominates the annual-mean response and leads to enhanced net precipitation in the hemisphere with the brighter summer.

By contrast, if the ascending branch is already located close to the pole, as it is in the simulation with Titan's rotation rate, the poleward shift and the associated strengthening of the Hadley circulation are limited by the size of the planet. What can then dominate instead is the length of summer: a dimmer but longer summer at aphelion may lead to an ascending branch of the Hadley circulation that is closer to the pole for a longer period. Thus, averaged over spring and summer (from equinox to equinox), the lengthening of the period with a solstitial circulation pattern in the dimmer summer overcompensates the strengthening of the circulation in the brighter summer, resulting in a stronger averaged Hadley circulation in the dimmer summer (Figures 2a and 2b). The same length-of-summer effect also amplifies the mean moisture transport toward the summer pole, because the solstitial moisture transport in a longer but dimmer summer is sustained for a longer period. This occurs in our simulations with Titan's rotation rate: The upward mass flux in the polar region around the dimmer summer solstice is slightly weaker, but the relatively strong solstitial moisture transport toward the summer pole is maintained for longer (Figure 3a). This overcompensates the weakened upward mass flux and moisture transport and leads to more annual-mean net precipitation in the hemisphere with the longer and dimmer summer (Figure 1).

5. Discussions and Conclusions

We have investigated the contrasting responses of atmospheres with Titan's and Earth's rotation rate to orbital precession in a setting with no prescribed hemispheric asymmetries in boundary conditions other than those associated with seasonal insolation variations. With Titan's rotation rate, annual-mean precipitation is stronger in the hemisphere with the dimmer but longer summer at aphelion. With Earth's rotation rate, annual-mean precipitation is stronger in the hemisphere with the brighter but shorter summer at perihelion. The key to understanding this difference is the different response of the dynamic component of methane transport to orbital precession. For slow rotation rates (such as Titan's), the ascending branch of the MMC around solstice is located close to the summer pole. By contrast, it is located at a lower latitudes for more rapid rotation rates (such as Earth's). An ascending branch close to the pole cannot respond to orbital precession by shifting farther poleward, limiting the degree to which the MMC strength and the moisture transport the MMC engenders can respond nonlinearly. Instead, moisture transport can react to the length of summer: strong (summertime) poleward moisture transport can occur for longer, leading to enhanced annual-mean moisture transport toward the pole with the dimmer but longer summer. An ascending branch in lower latitudes can respond to orbital precession by shifting farther poleward, leading to nonlinear

amplification of the MMC and to enhanced annual-mean moisture transport into the hemisphere with the brighter but shorter summer. This, ultimately, likely accounts for the hemispheric dichotomy in the methane distribution on Titan, with more surface methane near the north pole — the pole that currently has the dimmer but longer summer.

Acknowledgments
This work was supported by the NASA Outer Planets Research Program (grant NNX10AQ05G) and by the National Science Foundation (grant AGS-1049201). The program code for the Titan GCM is available at climate-dynamics.org. Simulation output is available from the authors upon request.

References

Aharonson, O., A. G. Hayes, J. I. Lunine, R. D. Lorenz, M. D. Allison, and C. Elachi (2009), An asymmetric distribution of lakes on Titan as a possible consequence of orbital forcing, *Nat. Geosci.*, *2*, 851–854.
Clement, A. C., A. Hall, and A. J. Broccoli (2004), The importance of precessional signals in the tropical climate, *Clim. Dyn.*, *22*, 327–341.
Cruz, F. W., S. J. Burns, I. Karmann, W. D. Sharp, M. Vuille, A. O. Cardoso, J. A. Ferrari, P. L. S. Dias, and O. Viana (2005), Insolation-driven changes in atmospheric circulation over the past 116,000 years in subtropical Brazil, *Nature*, *434*, 63–66.
Held, I. M., and A. Y. Hou (1980), Nonlinear axially symmetric circulations in a nearly inviscid atmosphere, *J. Atmos. Sci.*, *37*, 515–533.
Held, I. M., and B. J. Soden (2006), Robust responses of the hydrological cycle to global warming, *J. Clim.*, *19*, 5686–5699.
Herzschuh, U. (2006), Palaeo-moisture evolution in monsoonal Central Asia during the last 50,000 years, *Quat. Sci. Rev.*, *25*, 163–178.
Kutzbach, J. E., and P. J. Guetter (1986), The influence of changing orbital parameters and surface boundary conditions on climate simulations for the past 18,000 years, *J. Atmos. Sci.*, *43*, 1726–1759.
Lindzen, R. S., and A. Y. Hou (1988), Hadley circulation for zonally averaged heating centered off the equator, *J. Atmos. Sci.*, *45*, 2416–2427.
Lora, J. M., and J. L. Mitchell (2015), Titan's asymmetric lake distribution mediated by methane transport due to atmospheric eddies, *Geophys. Res. Lett.*, *42*, 6213–6220, doi:10.1002/2015GL064912.
Lora, J. M., J. I. Lunine, J. L. Russell, and A. G. Hayes (2014), Simulations of Titan's paleoclimate, *Icarus*, *243*, 264–273.
Lora, J. M., J. I. Lunine, and J. L. Russell (2015), GCM simulations of Titan's middle and lower atmosphere and comparison to observations, *Icarus*, *250*, 516–528.
Manabe, S. (1969), Climate and the ocean circulation: I. The atmospheric circulation and the hydrology of the Earth's surface, *Mon. Weather Rev.*, *97*(11), 739–774.
Merlis, T. M., T. Schneider, S. Bordoni, and I. Eisenman (2013a), Hadley circulation response to orbital precession. Part I: Aquaplanets, *J. Clim.*, *26*, 740–753.
Merlis, T. M., T. Schneider, S. Bordoni, and I. Eisenman (2013b), The tropical precipitation response to orbital precession, *J. Clim.*, *26*, 2010–2021.
Mitchell, J. L., R. T. Pierrehumbert, D. M. W. Frierson, and R. Caballero (2006), The dynamics behind Titan's methane clouds, *Proc. Natl. Acad. Sci. U.S.A.*, *103*, 18,421–18,426.
Ruddiman, W. F. (2013), *Earth's Climate: Past and Future*, 3rd ed., W. H. Freeman, New York.
Schneider, T. (2006), The general circulation of the atmosphere, *Ann. Rev. Earth Planet. Sci.*, *34*, 655–688.
Schneider, T., P. A. O'Gorman, and X. J. Levine (2010), Water vapor and the dynamics of climate changes, *Rev. Geophys.*, *48*, RG3001, doi:10.1029/2009RG000302.
Schneider, T., S. D. B. Graves, E. L. Schaller, and M. E. Brown (2012), Polar methane accumulation and rainstorms on Titan from simulations of the methane cycle, *Nature*, *481*, 58–61.
Schneider, T., T. Bischoff, and G. H. Haug (2014), Migrations and dynamics of the intertropical convergence zone, *Nature*, *513*, 45–53.
Tigchelaar, M., and A. Timmermann (2015), Mechanisms rectifying the annual mean response of tropical Atlantic rainfall to precessional forcing, *Clim. Dyn.*, *47*, 271–293, doi:10.1007/s00382-015-2835-3.
Walker, C. C., and T. Schneider (2005), Response of idealized Hadley circulations to seasonally varying heating, *Geophys. Res. Lett.*, *32*, L06813, doi:10.1029/2004GL022304.
Walker, C. C., and T. Schneider (2006), Eddy influences on Hadley circulations: Simulations with an idealized GCM, *J. Atmos. Sci.*, *63*(12), 3333–3350.
Wang, X., A. S. Auler, R. L. Edwards, H. Cheng, E. Ito, and M. Solheid (2006), Interhemispheric anti-phasing of rainfall during the last glacial period, *Quat. Sci. Rev.*, *25*, 3391–3403.
Wang, X., A. S. Auler, R. L. Edwards, H. Cheng, Y. Wang, X. Kong, E. Ito, and M. Solheid (2007), Millennial-scale precipitation changes in southern Brazil over the past 90,000 years, *Geophys. Res. Lett.*, *34*, L23701, doi:10.1029/2007GL031149.
Wang, Y., H. Cheng, R. L. Edwards, X. Kong, X. Shao, S. Chen, J. Wu, X. Jiang, X. Wang, and Z. An (2008), Millennial- and orbital-scale changes in the East Asian monsoon over the past 224,000 years, *Nature*, *451*, 1090–1093.

Erratum

In the originally published version of this article, several instances of text were incorrectly typeset. The following have been since been corrected, and this version may be considered the authoritative version of record.

In Figures 1 and 2, the degree symbol has been removed after "Latitude" and has been correctly added to the latitude labels (−60, −30, 0, 30, and 60).